South Asian Research Journal of Natural Products

Volume 7, Issue 3, Page 358-382, 2024; Article no.SARJNP.125919

Screening of Potential Cancer Inhibitors Using *Curcuma longa* (Turmeric) Extract through Molecular Docking, ADME and DFT Methods

Adindu Chinonso Blessing [a*], Kalu Georgina Ijeoma [a], Uche Godswill Nwokeke [a] and Ibe Frances Chizoruo [a]

[a] Department of Chemistry, Imo State University, Owerri, P M B 2000 Owerri, Imo State, Nigeria.

Authors' contributions

This work was carried out in collaboration among all authors. All authors read and approved the final manuscript.

Article Information

Open Peer Review History:
This journal follows the Advanced Open Peer Review policy. Identity of the Reviewers, Editor(s) and additional Reviewers, peer review comments, different versions of the manuscript, comments of the editors, etc are available here: https://www.sdiarticle5.com/review-history/125919

Original Research Article

Received: 26/08/2024
Accepted: 29/10/2024
Published: 05/11/2024

ABSTRACT

We herein report the cancer inhibition potentials of compounds extracted from *Curcuma longa* (Turmeric). The chemical contents were extracted in ethanol and chloroform respectively, analyzed with fourier transform infrared spectroscopy (FTIR) and gas chromatography mass spectrophotometry (GC-MS) techniques. The human progesterone receptor (4oar), epidermal growth factor receptor (4zau), and Human NUDT5 receptor (2dsd) were used as protein targets for the protein-ligand interaction using molecular docking method. Drug-like, pharmacokinetics, and pharmacodynamic properties were predicted using swissadme. Density functional theory (DFT) calculations were undertaken to relate the structures of the chemical constituents to their reactivities. The molecular docking results showed that the compounds identified in the

**Corresponding author: Email: blessingojiegbe@yahoo.com, blessingadindu@imsu.edu.ng;*

Cite as: *Blessing, Adindu Chinonso, Kalu Georgina Ijeoma, Uche Godswill Nwokeke, and Ibe Frances Chizoruo. 2024. "Screening of Potential Cancer Inhibitors Using Curcuma Longa (Turmeric) Extract through Molecular Docking, ADME and DFT Methods". South Asian Research Journal of Natural Products 7 (3):358-82. https://journalsarjnp.com/index.php/SARJNP/article/view/169.*

GC-MS analysis interacted perfectly with the drug targets, Cyclohexadecane, 1,2-diethyl-, lunamarin and Cyclopenteno[4.3-b]tetrahydrofuran, 3-[(4-methyl-5-oxo-3-phenylthio) tetrahydrofuran-2-yloxymethylene]- gave the highest negative binding energy with the 4oar cancer protein target $(-8.7\ K\ cal\ mol^{-1})$, lunamarin showed the best negative binding affinity $(-8.5\ K\ cal\ mol^{-1})$ in the 4azu cancer protein while Benzo[h]quinoline, 2,4-dimethyl- showed the highest negative binding affinity $(-7.6\ K\ cal\ mol^{-1})$ in 2dsd protein. SwissADME prediction results showed that the compounds have good pharmacokinetics, and pharmacodynamic properties: none of them violated more than one of Lipinski's rule, DFT calculations showed good relationship between the compounds and their reactivities. The results obtained from the experiments revealed that compounds contained in *Curcuma longa* could exert positive effects towards the inhibition of cancer cells.

Keywords: Cancer; turmeric; molecular docking, density functional theory, lipinski.

1. INTRODUCTION

Cancer is one of the world's life-threatening diseases, and leading cause of death in humans. It is the second most deadly diseases around the world [1,2]. Cancer is an illness that starts with genetic and epigenetic changes occurring in specific cells, and some of them can spread and migrate to other tissues in the body [3]. It occurs as a result of genetic cell damage which show division difficulty and mutation [4]. Cancer is named depending on the part of the body affected hence we have prostate cancer, lung cancer, breast cancer, brain cancer e. t. c.

Prostate cancer occurs when the prostate gland in men grows out of control and becomes malignant [5]. Lung cancer is the type that begins as a malignant growth in the lungs. People involved in cigarette smoking are at greater risk of contracting lung cancer.

Breast cancer is one of the most lethal diseases found in women, it presents symptoms such as change in breast shape, a lump growing in the breast, fluid from the nipple, skin dimpling and scaly or red patch of skin [6] depending on the type, stage and the age of the patient. It is the leading type of cancer in women [7]. Most cancer treatment methods show adverse side effects and drug resistance.

Molecular docking is a computer simulation method used in drug discovery to predict the binding procedures of ligands on protein targets. Bioactive materials called nutraceuticals, found in food sources such as turmeric can be used in the treatment of several diseases. Sourcing for molecular targets can help in the formation of disease-specific new therapies [8]. Nutraceuticals are natural food substances with therapeutic effects on human health that are found in dietary sources [9]. Molecular docking enables one to predict the binding affinity of nutraceuticals (ligands) with protein targets.

Density functional theory is a computational chemistry method used to calculate electronic structures, it gives the most precise and reliable results for material systems [10], which can be compatible with experimental results.

Previously 90 % of drug failure was due to poor pharmacokinetic profiles [11,12], poor drug toxicity management and lack of drug likeness data [13] in view of these difficulties the efforts in drug developments have focused on improving the process of discovery of drugs by evaluating their absorption, distribution, metabolism, and elimination (ADME) properties of molecules in the early stages of drug production [14]. The present work tries to ascertain the bioactive components of *Curcuma longa* (Turmeric) and screen them for their cancer inhibiting properties using molecular docking method.

2. MATERIALS AND METHODS

2.1 Procurement of Reagents and Plant Material

Analytical grade reagents were used throughout the experiments, procured from a renowned reagent dealer in Owerri Imo State Nigeria. The *Curcuma longa* (Turmeric) rhizomes used in this project were harvested from the botanical garden of the Imo state university Owerri, sun dried, ground to powdered form using mortar and pestle. 400 g of the powder was soaked in 1 L of absolute ethanol and chloroform respectively and left for 72 h [15], the mixture was filtered with whatman grade 1 cellulose filter paper of size 580 x 680 mm the filtrate was concentrated and submitted for Fourier transform infrared spectroscopy and Gas Chromatography -Mass Spectrophotometry examinations.

2.2 Phytochemical Screening

To ascertain the functional groups present in the plant extract, FTIR analysis was performed. The analysis was done using SHIMADZU Model number 84008 at the facilities of the National research institute, Zaria Kaduna State Nigeria [16]. Phytochemical identification was done by GC-MS screening using an Agilent 19091S-433UI GCMS model with parameters HP-5ms Ultra Inert 0 °C—325 °C (350 °C): 30 m x 250 µm x 0.25 at the Amadu Bello university research laboratory. The obtained result was compared with the National Institute of Standards and Technology (NIST) mass spectral library [17].

2.3 Ligand Identification and Characterizations

The 3-Dimensional structure-data files (SDF) of the identified compounds were sourced and downloaded from pubchem online database and used as the ligands for the molecular docking interaction. The ligands were minimized in PYRX online virtual screening tool with a universal force field at step 200 [18].

2.4 Identification and Preparation of Target

Three cancer protein targets, the human progesterone receptor (4oar), epidermal growth factor receptor (4zau), and Human NUDT5 receptor (2dsd) were identified from literature [19-21] and downloaded from protein databank. The amino acids in the active site of the 4aor protein include GLN 718, ASN 719, GLU 723, GLN 725, LEU 797, GYS 891 and THK 894, for the 4zau protein, the amino acids of the active site are VAL 726, ALA743, MET 793, PRO 794, GLY 796 and CYS 797 and 2dsd has active site amino acids as TPR 28, THR 45, TRP 46, GLN 82, GLN 97, ALA 96, LEU 98, GLU 112, GLU 113, GLU 116 and GLU 166. protein preparation was achieved by uploading the proteins to Biovia discovery studio where the co-crystallized ligand and the interfering crystallographic water molecules were respectively removed. The proteins were then saved as protein data bank files and used as the macromolecule in PYRX software for the molecular docking analysis.

2.5 Molecular Docking Analysis

Molecular docking to give a prediction of the ligand-receptor complex, was performed using the autodock vina found in PYRX visual screening molecular docking tool. The molecular docking analysis was achieved through two main interrelated steps: the first step was by sampling the conformations of the ligands in the active site of the target protein and the second is the ranking the conformations through a scoring function. The drug control used for the docking procedure was Abemaciclib, a drug used effectively for the control of cancer [22]. Post docking analysis was performed using the Biovia discovery studio [23] where the docking interactions were visualized.

2.6 Drug Properties Examination

The compounds with docking scores lower than $-7.6\ Kcal\ mol^{-1}$ were selected and submitted to SwissADME (http://swissadme.ch/) to estimate ligands' drug-likeness, physicochemical properties, pharmacokinetics, and medicinal chemistry friendliness characteristics. The canonical simplified molecular input line entry system (smiles) of the identified compounds were obtained from pubchem online database and submitted to SwissADME (http://swissadme.ch/) [24] for the adme analysis. The properties predicted were partition coefficient between n-octanol and water (log Po/w), water solubility, human gastrointestinal absorption (HIA), blood-brain barrier (BBB), drug-likeness and total polar surface area (TPSA).

2.7 Density Functional Theory Calculations

Calculation of highest occupied molecular orbitals (HOMO) and lowest occupied molecular orbitals (LUMO) energies were performed using Acceryl material studio 7.0 software [16]. Geometric optimization in the Dmol3 tool of the material studio software was performed prior to the calculations.

3. RESULTS

3.1 Fourier Transform Infrared Spectroscopy (FTIR) Results

FTIR examination was performed on the *Curcuma longa* powder and the spectrum is presented in Fig. 1 while the functional groups present are given in Table 1.

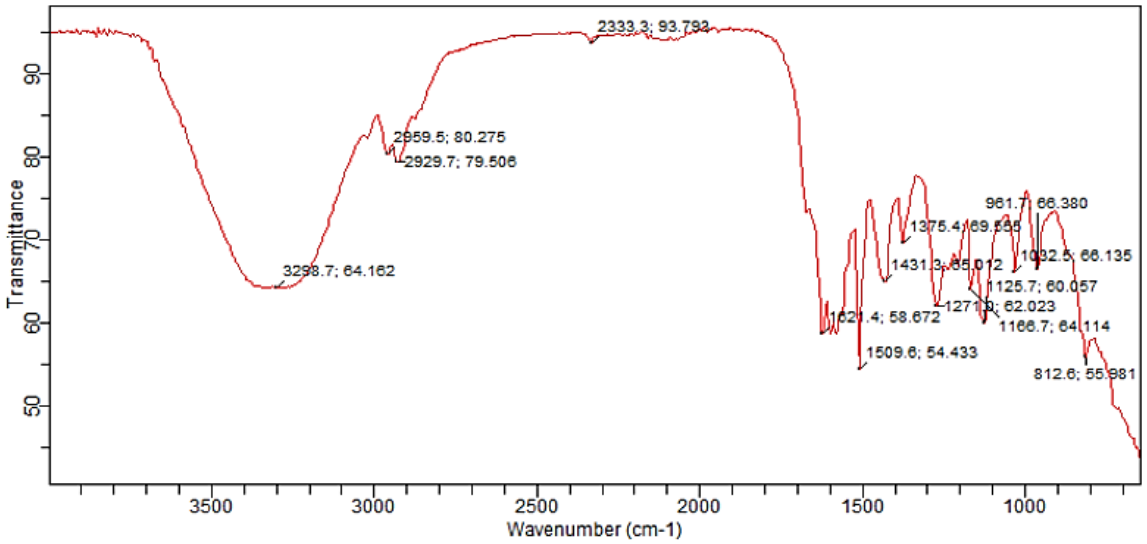

Fig. 1. FTIR spectrum of the *Curcuma longa* powder

Table 1. Functional groups found in the *Curcuma longa* powder

S/No.	Wavenumber $(\mathbf{cm^{-1}})$	Functional group
1.	3298.7	OH of alcohol
2.	2959.5, 2929.7	CH stretch
3.	2333.3	C-C
4.	1621.4	C=C
5.	1509.	

The functional groups present indicated that the plant would be a good disease reducing material [16].

3.2 Gas Chromatography- Mass Spectrophotometry Result

GC-MS analysis was performed on the plant extract and the chromatogram from the ethanol extract is presented in Fig. 2 (a) whereas that from the chloroform extract is presented in Fig. 2 (b). Tables 2 and 3 show the compounds present in the ethanol and chloroform extracts respectively. Mass spectrum of some of the identified compounds are presented in Fig. 3.

3.3 Molecular Docking Result

To ascertain the Target-ligand interaction between the targets and the identified compounds, molecular docking procedure was undertaken. The compounds exhibited varying degrees of binding on the binding packets of the cancer proteins as shown by the changes in the free energies (ΔG) values of the compounds. Table 4 presents the docking free energies of some of the compounds with good binding affinities and the drug control while Fig. 4 shows the 3D and 2D protein ligand interactions of the selected compounds. Whereas, Cyclohexadecane, 1,2-diethyl-, lunamarin and Cyclopenteno[4.3-b]tetrahydrofuran, 3-[(4-methyl-5-oxo-3-phenylthio) tetrahydrofuran-2-yloxymethylene]- showed the highest negative binding affinity $(-8.7\ K\ cal\ mol^{-1})$ in the 4aor cancer protein surpassing even the control ligand Abemaciclib $(-8.3\ K\ cal\ mol^{-1})$, in the 4zau protein, lunamarin gave the best negative binding affinity $(-8.5\ K\ cal\ mol^{-1})$ again surpassing the control ligand $(-8.2\ K\ cal\ mol^{-1})$, Benzo[h]quinoline, 2,4-dimethyl- gave the highest negative binding affinity $(-7.6\ K\ cal\ mol^{-1})$ in 2dsd cancer protein and this is very close to the control ligand $(-7.7\ K\ cal\ mol^{-1})$. The findings from this work suggest that these compounds could have positive effect on cancer cell inhibition when isolated from turmeric, Cyclohexadecane, 1,2-diethyl-, lunamarin and Cyclopenteno[4.3-b]tetrahydrofuran showed good interaction with GLN 725 at the active site of the 4oar protein

with Cyclopenteno[4.3-b]tetrahydrofuran showing more similar interaction at the active site by binding with LEU 718, CYS 891, LEU 797 and CYS 891 amino acids. In the 4zau protein, lumarin sowed similar interaction with the amino acid of the active site by binding to ALA 743, GLY 796, MET 793 and GLY 796, for the 2dsd protein Benzo[h]quinoline, 2,4-dimethyl- did not show similar binding to the active site amino acids.

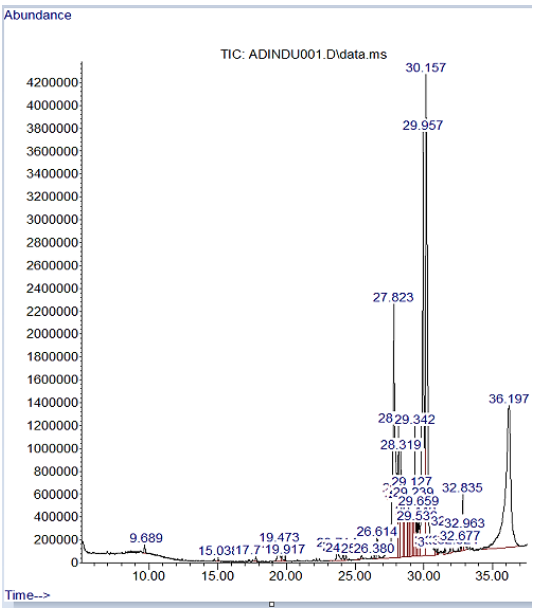

Fig. 2(a). Chromatogram of the ethanol extract of *Curcuma longa*

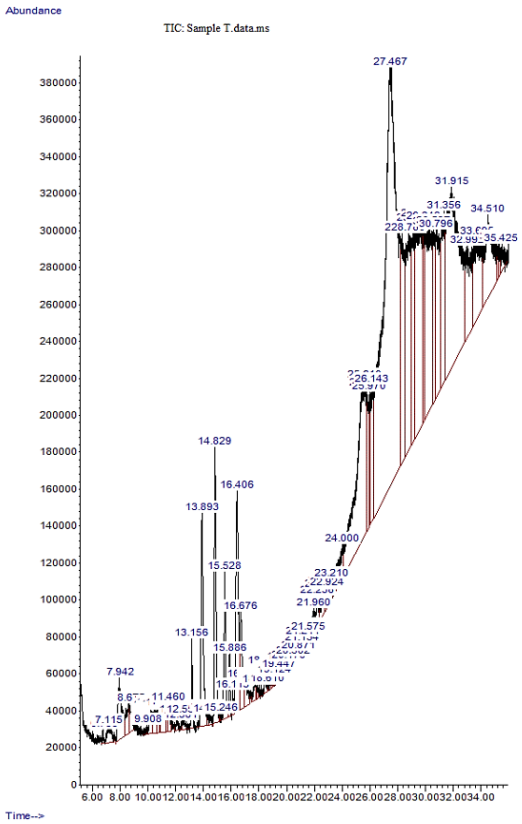

Fig. 2(b). Chromatogram of the chloroform extract of Curcuma *longa*

Table 2. Compounds obtained from theGC-MS result of the ethanol extract of *Curcuma longa* and Abemaciclib (control)

S/No.	Area %	Name	Structure	Pubchem Cid
1.		Abemaciclib	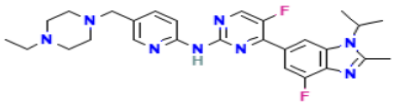	46220502
2.	0.1796	Hydroxylamine, O-decyl-		34704
3.	0.0632	Tetradecane		12389
4.	0.0927	Nonanoic acid, methyl ester		15606
5.	0.806	Dodecanoic acid		3893
6	0.1496	Pentadecafluorooctanoic acid, undecyl ester	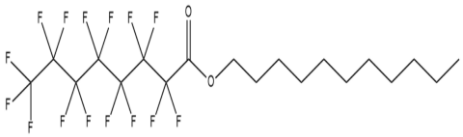	91691494
7	0.0998	Hexadecane		11006
8	0.6083	Tetradecanoic acid	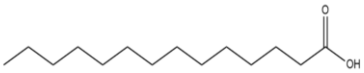	11005
9	0.1609	1-Docosene		74138
10	0.1116	Octadecane		11635
11	0.1131	9-Heptadecanone	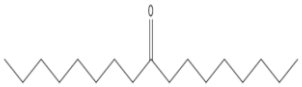	10887
12	0.0643	Pentadecane, 1-bromo-		12394

S/No.	Area %	Name	Structure	Pubchem Cid
13	0.4599	Hexadecanoic acid, methyl ester		8181
14	15.0006	n-Hexadecanoic acid		985
15	4.0392	Cyclohexadecane, 1,2-diethyl-	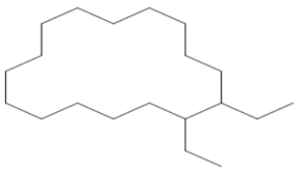	536940
16	4.1349	Sulfurous acid, 2-propyl tetradecyl ester		6420356
17	2.0913	trans-4-Aminocyclohexanol, N,O-diacetyl	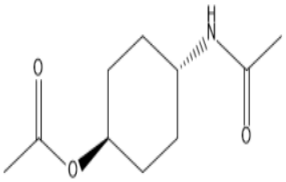	15442390
18	4.5046	Cycloeicosane	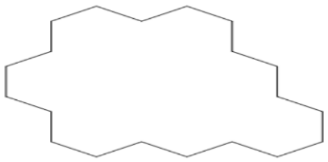	520444
19	21.3648	Oleic Acid	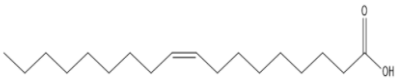	445639
20	1.4073	Decyl oleate	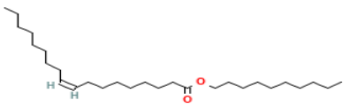	5363234
21	1.172	10-Heneicosene (c,t)	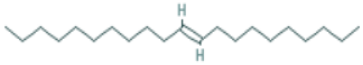	5364553
22	2.1509	cis-13-Octadecenoic acid, methyl ester		12541027
23	0.7336	1-Eicosene		18936

S/No.	Area %	Name	Structure	Pubchem Cid
24	0.819	Heneicosane		12403
25	0.9099	Methyl stearate		8201
26	15.5534	cis-Vaccenic acid		5282761
27	20.4201	Octadecanoic acid		5281
28	0.1645	Cyclopentane, 1-methyl-3-(1-methylethyl)-	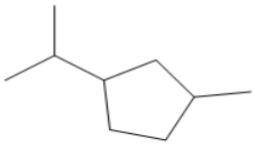	521465
29	0.0524	Carbonic acid, hexadecyl prop-1-en-2-yl ester		91692933
30	0.1329	1-Decanol, 2-hexyl-	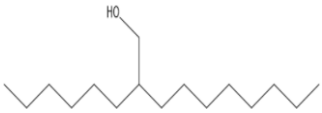	95337
31	0.0558	4-Cyanobenzoic acid, dodecyl ester	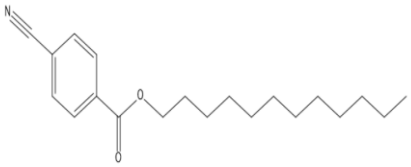	531621
32	0.4526	Hexadecanoic acid, 2-hydroxy-1-(hydroxymethyl)ethyl ester		123409
33	0.0645	Z-8-Methyl-9-tetradecenoic acid	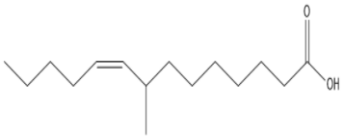	5364410

S/No.	Area %	Name	Structure	Pubchem Cid
34	0.0919	1-Decanol, 2-hexyl-	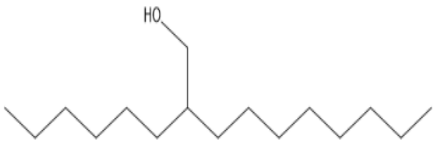	95337
35	0.1243	Cinnamyl cinnamate	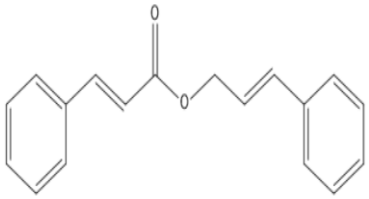	1550890
36	1.1133	9-Octadecenal, (Z)-		5364492
37	0.5373	Cetene		12395

Table 3. Compounds obtained from the GC-MS result of the chloroform extract of *Curcuma longa*

S/No	Area %	Name	Structure	Pubchem Cid
1.	0.31	2-Fluorobenzyl alcohol	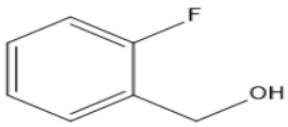	67969
2.	0.22	Butanoic acid, 3-hydroxy-, ethyl ester	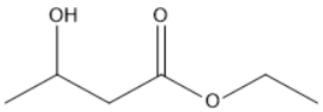	62572
3	0.30	2H-Azepin-2-one, hexahydro-1-(hydroxymethyl)-	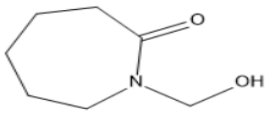	83127
4	0.05	6-Acetyl-.beta.-d-mannose	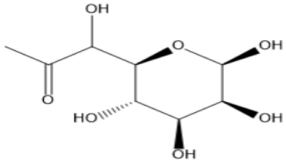	249901862
5	0.45	Undec-10-ynoic acid, undecyl ester		91692431
6	0.21	Cyclononene		5463153

S/No	Area %	Name	Structure	Pubchem Cid
7	0.10	Dodecyl propyl ether		110199
8	0.11	Decanoic acid, 2,3-dihydroxypropyl ester	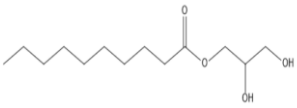	92926
9	0.30	Undecylenic acid		5634
10	2.01	n-Hexadecanoic acid		985
11	0.29	d-Lyxose	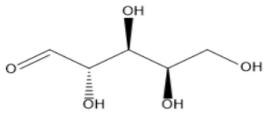	439240
12	0.02	Cyclopentadecanone, 2-hydroxy-	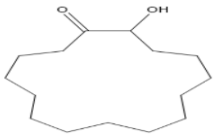	543400
13	0.38	Hexadecanoic acid, methyl ester		8181
14	0.05	Z,Z-4,16-Octadecadien-1-ol acetate		5364627
15	0.09	3-Dodecen-1-ol		5364625
16	1.93	(S,Z)-Heptadeca-1,9-dien-4,6-diyn-3-ol	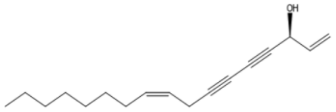	5469789
17	0.32	9-Octadecenal		5283381
18	1.05	11-Octadecenoic acid, methyl ester		5364432
19	0.31	Methyl stearate		8201
20	0.19	cis-9,10-Epoxyoctadecan-1-ol		12550092

S/No	Area %	Name	Structure	Pubchem Cid
21	2.40	cis-13-Octadecenoic acid		5312441
22	0.95	Octadecanoic acid	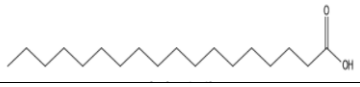	5281
23	0.76	Cyclopropaneoctanal, 2-octyl-		550143
24	0.19	11-Dodecen-1-ol trifluoroacetate	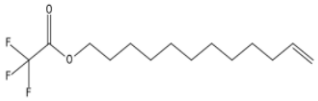	543399
25	0.60	1,3,12-Nonadecatriene		548894
26	0.80	445639		445639
27	0.16	E-11-Hexadecenal		5283376
28	0.01	9,17-Octadecadienal, (Z)-		5365667
29	0.34	(Z)-Tetradec-11-en-1-yl 2,2,2-trifluoroacetate		5364636
30	0.456	9-Octadecenoic acid, (E)-		637517
31	0.01	6-Octadecenoic acid, (Z)-		5281125
32	0.16	1-Cyclohexylnonene	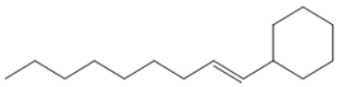	5364533
33	0.36	Propyleneglycol monoleate	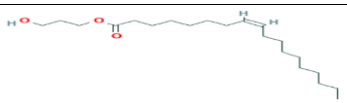	5365625
34	0.34	9-Octadecenoic acid (Z)-, 2-hydroxy-1-(hydroxymethyl)ethyl ester	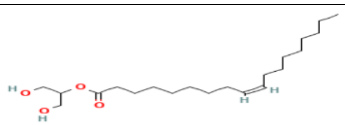	5319879

S/No	Area %	Name	Structure	Pubchem Cid
35	6.49	Acetamide, 2-chloro-N-(3-cyano-4,6-dihydro-4,4,6,6-tetramethylthieno[2,3-c]furan-2-yl)-	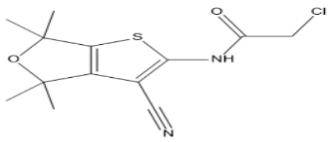	5303086
36	6.72	Anthracene, 9-(2-propenyl)-	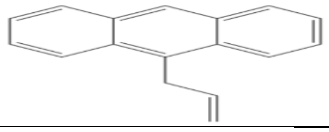	612797
37	26.32	1H-Indene, 2-butyl-5-hexyloctahydr-o	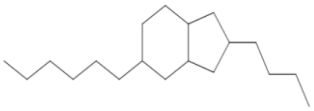	278087
38	0.77	Pyridine-3-carboxamide, oxime, N-(2-trifluoromethylphenyl)-	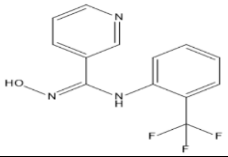	550559
39	1.35	2,6-Lutidine, 3,5-dichloro-4-cyclohexylthio	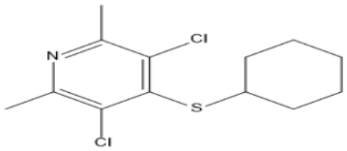	544007
40	3.28	2-Ethylacridine	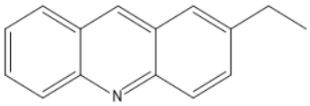	610161
41	9.30	Thymol, TBDMS derivative	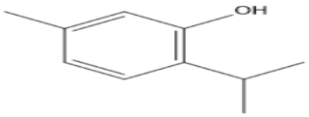	6989
42	5.19	Caryophyllene	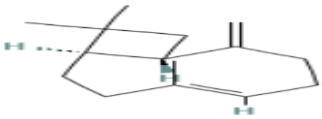	5281515
43	1.41	Demecolcine	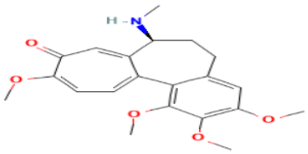	220401
44	2.95	Benzo[h]quinoline, 2,4-dimethyl-	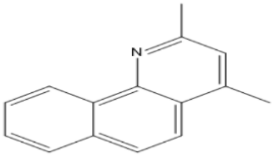	610182
45	2.86	6-Chloro-1-ethyl-4-oxo-N-(pyridin-4-ylmethyl)quinoline-3-carboxamide	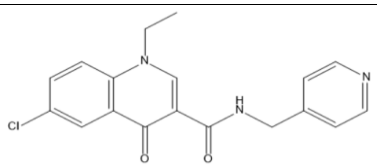	30132216

S/No	Area %	Name	Structure	Pubchem Cid
46	9.82	Lunamarin	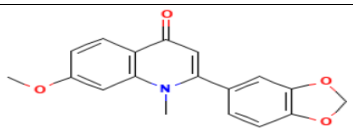	442922
47	2.30	Cyclopenteno[4.3-b]tetrahydrofuran, 3-[(4-methyl-5-oxo-3-phenylthio) tetrahydrofuran-2-yloxymethylene]-	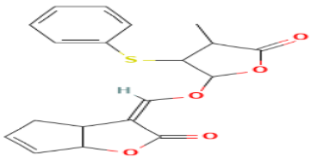	5375838
48	2.59	Propanamide, N-(3-methoxyphenyl)-2,2-dimethyl-	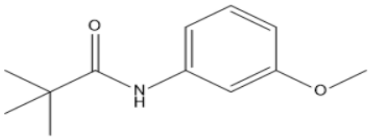	546358
49	2.63	Catechin	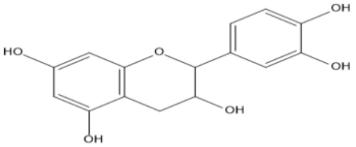	9064
50	0.17	1H-Indole-2-carboxylic acid, 6-(4-ethoxyphenyl)-3-methyl-4-oxo-4,5,6 ,7-tetrahydro-, isopropyl ester	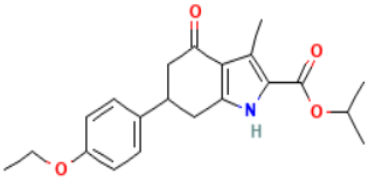	4916205

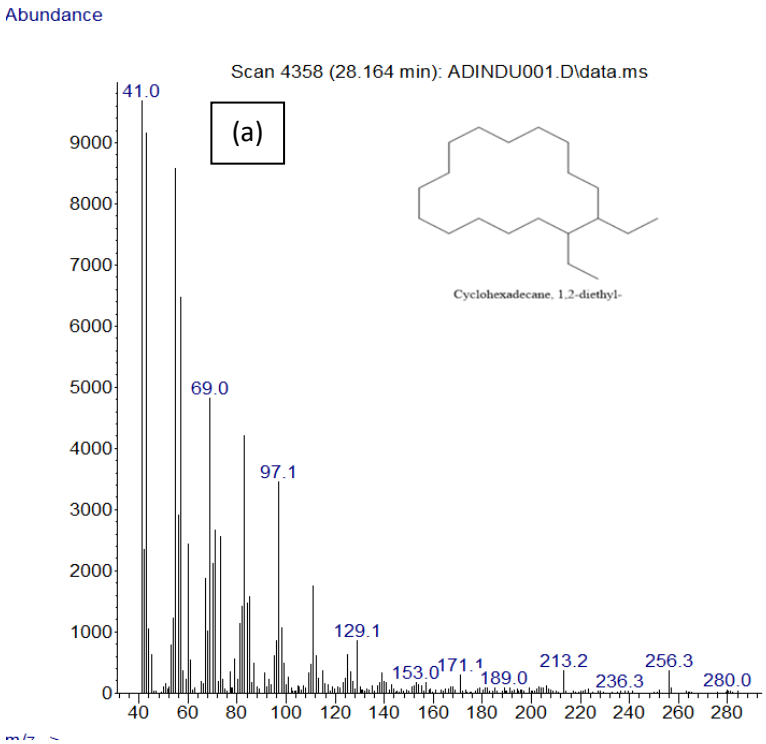

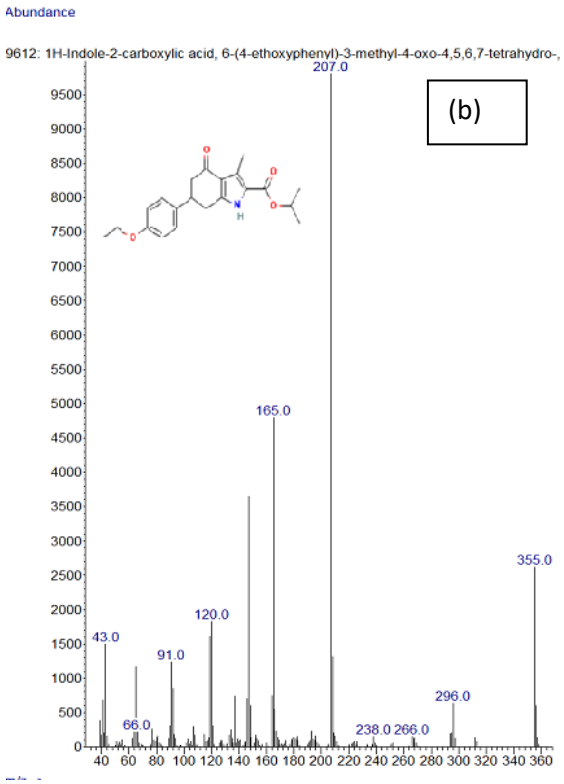
Abundance
9612: 1H-Indole-2-carboxylic acid, 6-(4-ethoxyphenyl)-3-methyl-4-oxo-4,5,6,7-tetrahydro-,
(b)
207.0
165.0
355.0
120.0
43.0
91.0
296.0
66.0
238.0
266.0
m/z-->

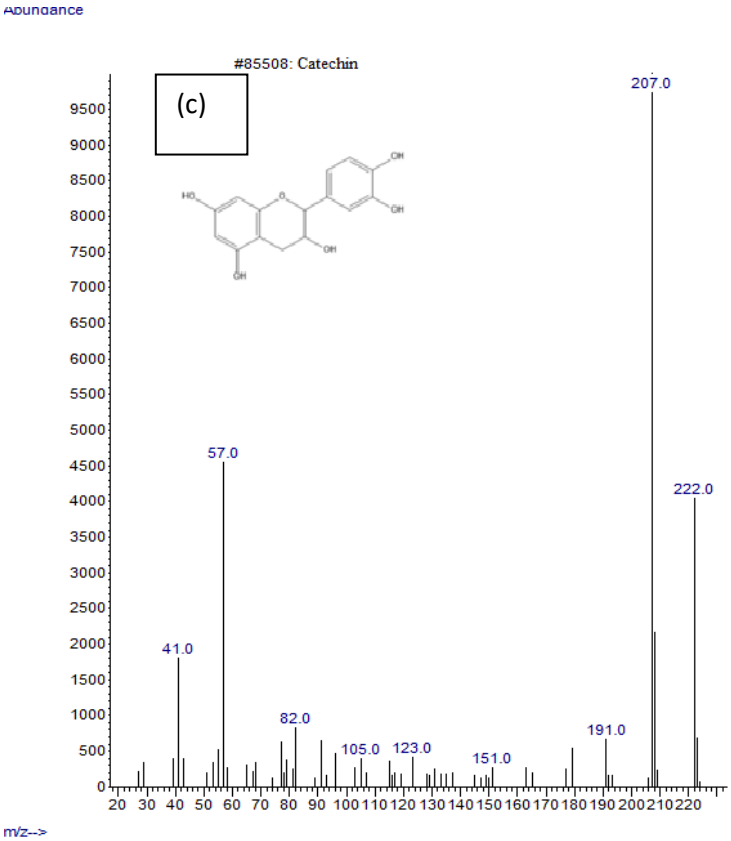
Abundance
#85508: Catechin
(c)
207.0
57.0
222.0
41.0
82.0
191.0
105.0
123.0
151.0
m/z-->

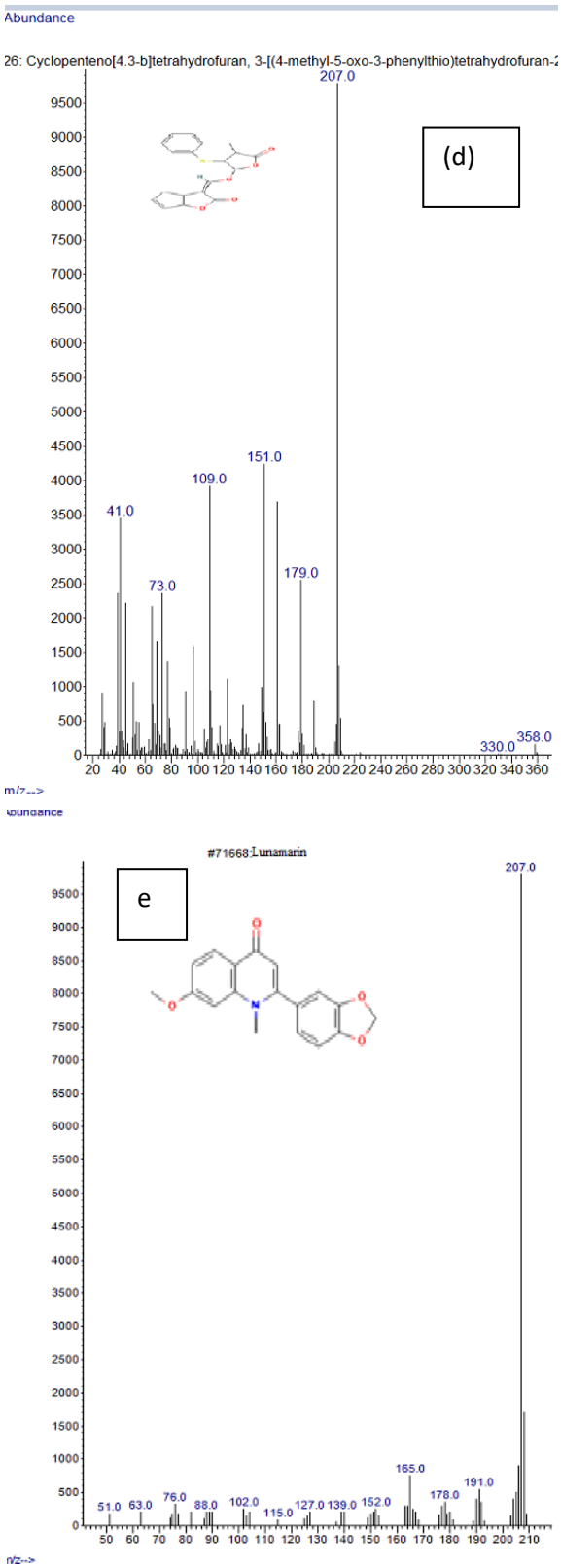

Fig. 3. Mass spectrum of (a) Cyclohexadecane, 1,2-diethyl- (b) 1H-Indole-2-carboxylic acid, 6-(4- ethoxyphenyl)-3-methyl-4-oxo-4,5,6 ,7-tetrahydro-, isopropyl ester (c) Catechin (d) Cyclopenteno[4.3-b]tetrahydrofuran, 3-[(4-methyl-5-oxo-3-phenylthio) tetrahydrofuran-2-yloxymethylene]- and (e) Lunamarin

Table 4. Docking scores of some of the compounds with good docking scores

S/No	Name of compound	Pubchem icd	Docking scores ($Kcal\ mol^{-1}$)		
			4oar	4zau	2dsd
1	Abemaciclib	46220502	-8.3	-8.2	-7.7
2	Cycloeicosane	520444	-7.2	-7.6	-7.4
3	Cyclohexadecane, 1,2-diethyl-	536940	-8.7	-7.5	-6.7
4	Cinnamyl cinnamate	1550890	-7.2	-6.7	-7.1
5	1H-Indole-2-carboxylic acid, 6-(4-ethoxyphenyl)-3-methyl-4-oxo-4,5,6 ,7-tetrahydro-, isopropyl ester	4916205	-8.4	-8.2	-7.4
6	Catechin	9064	-8.4	-7.8	-7.2
7	Cyclopenteno[4.3-b]tetrahydrofuran, 3-[(4-methyl-5-oxo-3-phenylthio) tetrahydrofuran-2-yloxymethylene]-	5375838	-8.7	-7.5	-6.8
8	Lunamarin	442922	-8.7	-8.5	-7.0
9	6-Chloro-1-ethyl-4-oxo-N-(pyridin-4-ylmethyl)quinoline-3-carboxamide	30132216	-7.7	-7.3	-6.6
10	Benzo[h]quinoline, 2,4-dimethyl-	610182	-7.8	-7.3	-7.6
11	Demecolcine	220401	-5.7	-7.1	-6.2
12	Caryophyllene	5281515	-7.4	-6.5	-6.7
13	2-Ethylacridine	610161	-7.7	-7.3	-7.5
14	Pyridine-3-carboxamide, oxime, N-(2-trifluoromethylphenyl)-	550559	-7.3	-6.8	-6.7
15	Anthracene, 9-(2-propenyl)-	612797	-7.9	-7.2	-7.0
15 16	Cyclopentadecanone, 2-hydroxy-	543400	-6.3	-6.6	-6.8
17	Propanamide, N-(3-methoxyphenyl)-2,2-dimethyl-	546358	-6.5	-5.9	-5.7
18	Thymol, TBDMS derivative	6987	-6.0	-5.7	-5.4
19	1H-Indene, 2-butyl-5-hexyloctahydr-o	278087	-6.2	-6.6	-5.6
20	Acetamide, 2-chloro-N-(3-cyano-4,6-dihydro-4,4,6,6-tetramethylthieno[2,3-c]furan-2-yl)-	5303086	-7.1	-6.3	-5.8
21	1-Cyclohexylnonene	5364533	-6.6	-5.7	-4.9
22	Cyclononene	5463153_	-6.0	-4.7	-5.3

S/No	Name of compound	3D and 2D Interaction 4aor	4zau	2dsd
46220502	Abemaciclib	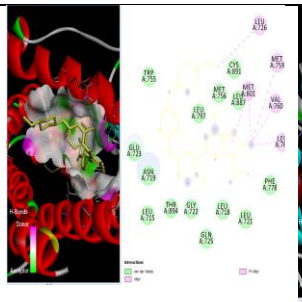	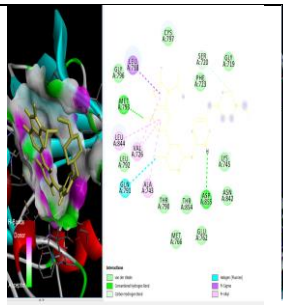	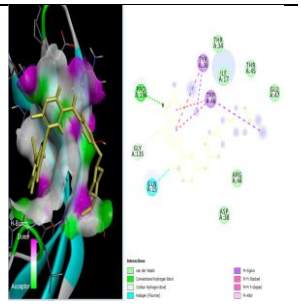

S/No	Name of	3D and 2D Interaction
536940	Cyclohexadecane, 1,2-diethyl-	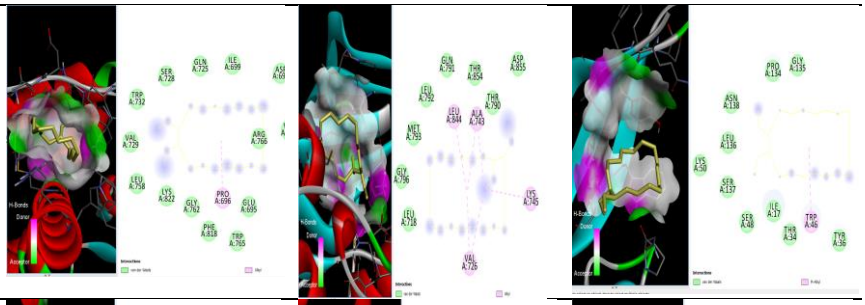
4916205	1H-Indole-2-carboxylic acid, 6-(4-ethoxyphenyl) -3-methyl-4-oxo-4,5,6 ,7-tetrahydro-, isopropyl ester	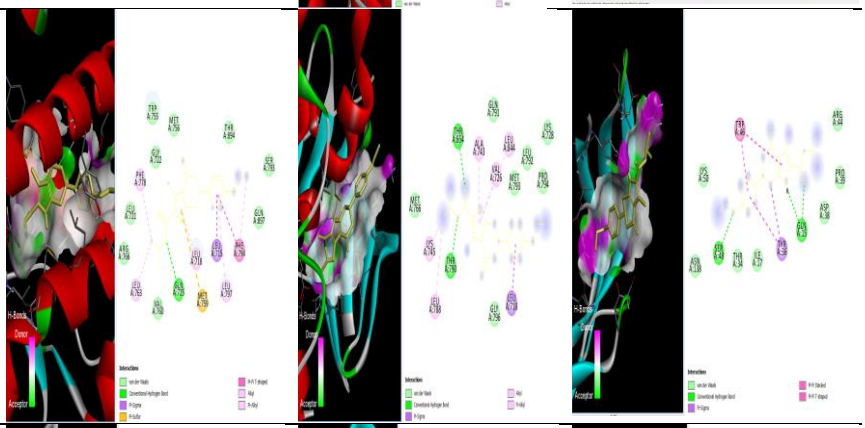
9064	Catechin	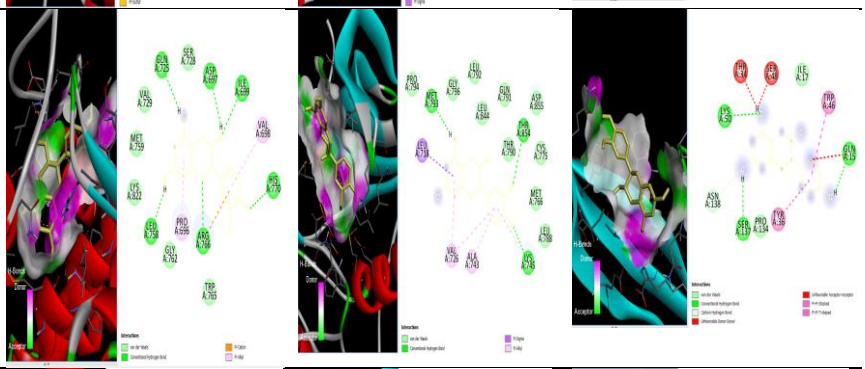
5375838	Cyclopentenon[4.3-b]tetrahydrofuran, 3-[(4-methyl-5-oxo-3-phenylthio) tetrahydrofuran-2-yloxymethylene]-	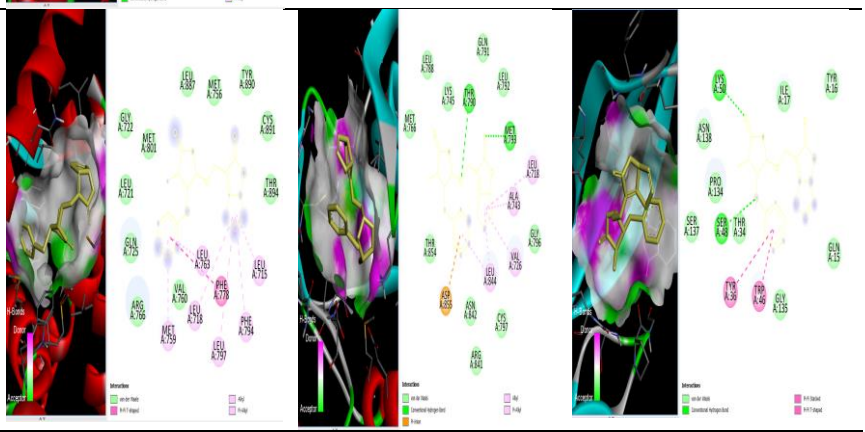

S/No	Name of	3D and 2D Interaction
442922	Lunamarin	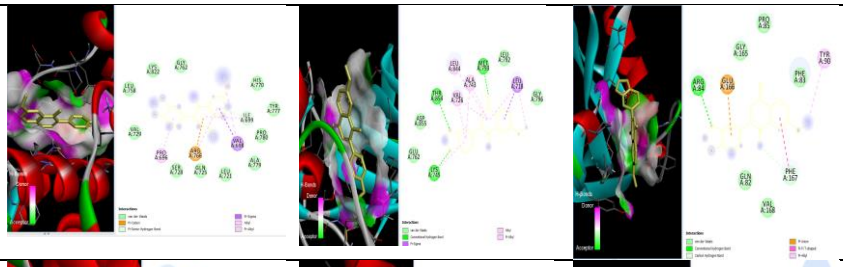
610182	Benzo[h]quinoline, 2,4-dimethyl-	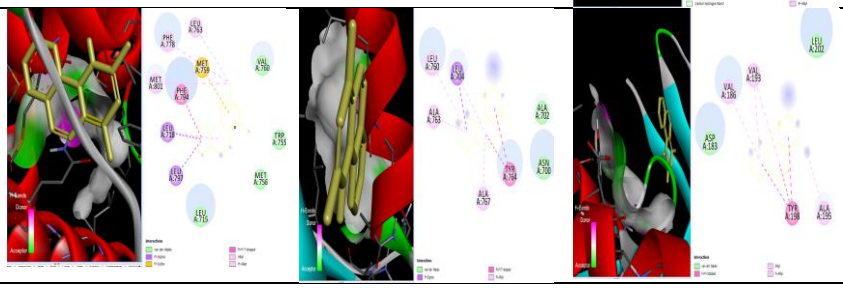

Fig. 4. 3D and 2D protein-ligand interactions of some of the selected compounds

Table 5. ADME properties of the selected compounds

Compound	NRA	HBA	HBD	Log K_p (cm/s)	TPSA (Å²)	Log *S* (ESOL)	HIA	BBB	Lipinski violations	Log $P_{o/w}$
Abemaciclib	7	8	1	-6.66	75.00	-5.36	High	No	1	4.04
Cyclohexadecane, 1,2-diethyl-	2	0	0	-0.73	0.00	-7.90	Low	No	1	6.96
1H-Indole-2-carboxylic acid, 6-(4-ethoxyphenyl)-3-methyl-4-oxo-4,5,6 ,7-tetrahydro-, isopropyl ester	6	4	1	-5.68	68.39	-4.44	High	yes	0	3.85
Catechin	1	6	5	-7.82	110.38	-2.22	High	No	0	0.83
Cyclopenteno[4.3-b]tetrahydrofuran, 3-[(4-methyl-5-oxo-3-phenylthio) tetrahydrofuran-2-yloxymethylene]-	4	5	0	-6.00	87.13	-4.18	High	No	0	2.92
Lunamarin	2	4	0	-5.97	49.69	-4.11	High	Yes	0	2.87

NRA-Number of rotatable bonds, HBA-Number of hydrogen bond acceptor, HBD-Number of hydrogen bond donor, TPSA-topological polar surface area, HIA- human gastrointestinal absorption, BBB- blood-brain barrier HBDNumber of hydrogen bond donor, NRB-Number of rotatable bond, logp=n-octanol/w

3.4 Drug Properties Result

To identify the molecules with best chances of becoming effective drugs for human consumption, swissADME evaluation was executed. The said molecule is expected to exhibit good biological activities. The result is presented in Table 5. One of the properties tested was the skin permeability coefficient (Kp) [25]. More negative values of log Kp (with Kp in cm/s), shows that the molecule will be less permeant to the skin, another important parameter predicted is the topological polar surface area (TPSA) which is used to estimate the membrane permeability efficacy of a compound, the range of value for the property is $20\ \text{Å} < \text{TPSA} < 130\ \text{Å}$. Interestingly only one of the molecules studied falls outside this range.

The water solubility parameter (log *S* (ESOL)) was also estimated, soluble molecules aids drug development processes [26], it is the property that determines drug absorption, the range of values for log *S* (ESOL) is $-6 < S\,(\text{ESOL})) < 0$ again only one of the compounds falls outside this range and five falls withing the range showing that they would be highly soluble in water and easily absorbed as drug samples.

The human gastrointestinal absorption (HIA) and blood-brain barrier (BBB) were also predicted. HIA [27] is a vital parameter for predicting the movement of the drugs to their targets, compounds having positive HIA are easily absorbed via the gastrointestinal tract when administered in oral form, one of the compounds studied has negative HIA while others have high HIA, the blood brain barrier (BBB) penetration screening showed that 4 of the compounds have negative penetration while 2 have positive penetration. The BBB regulates the drug permeability into the brain. The swissADME results showed that the compounds studied would serve as good drug candidates when administered in the correct dosage, none violated more than one of Lipinski's rules [16].

3.5 Density Functional Theory Result

To corelate the structures of the compounds to their reactivity, density functional theory calculations were undertaken, Calculations were done using the electronic structure program DMol3 in the framework of the Mulliken population analysis, the DND basis set and the Perdew-Wang (PW) local correlation density functional [28] whereas Fig. 5 depicts the optimized structures, frontier molecular orbitals and funki functions of some of the compounds with good inhibition ability, Table 6 represents the quantum chemical descriptors derived from the frontier molecular orbitals including the ionization potential (I), electron affinity (A), energy gap $(\mathrm{E_{LUMO}} - \mathrm{E_{HOMO}})$, absolute hardness (η), softness (δ), absolute electronegativity (χ) and electrophilicity (ω), The HOMO and LUMO molecular orbitals also known as the frontier orbitals describe the most reactive sites in the compound and they show the reactivity patterns of the molecule, whereas the HOMO orbital is an electron rich center waiting to donate to an electron deficient center , the LUMO orbital is an electron deficient environment waiting to accept electron from an electron rich center. The value of the energy gap $(\mathrm{E_{LUMO}} - \mathrm{E_{HOMO}})$ describes the chemical reactivity of the molecule, low values of $(\mathrm{E_{LUMO}} - \mathrm{E_{HOMO}})$ shows that the molecule can easily transfer electron and improves chemical reactivity [29]. The softness and hardness of a molecule describe the behavior of a molecule, while soft molecules show low resistance to change of electronic distribution during a chemical reaction, hard molecules show a high resistance to change of their electronic distribution in a reaction. The ionization potential describes the energy required to remove an electron from the ground state of the molecule while the electron affinity is the energy given off when a molecule in its ground state gains an electron, electronegativity is the ability of the molecule to attract an electron to itself. Electrophilicity (ω) is a factor that describes the electrophilic nature of a molecule; it predicts the propensity of a chemical specie to attract an electron to itself, with high values of electrophilicity characterizing good electrophilicity in a compound. The values of quantum chemical descriptors obtained in this study are comparable to what is obtained elsewhere [30,31] for diseases inhibition study showing that compounds from *Curcuma longa* could be good inhibitors of cancer cells.

The expressions used to calculate the quantum chemical descriptors are as below:

$$\mathrm{I} = -\mathrm{E_{HOMO}} \quad (1)$$

$$\mathrm{A} = -\mathrm{E_{LUMO}} \quad (2)$$

$$\Delta E = (\mathrm{E_{LUMO}} - \mathrm{E_{HOMO}}) \quad (3)$$

$$\eta = \frac{I-A}{2} \quad (4)$$

$$\delta = \frac{1}{\eta} \quad (5)$$

$$\chi = \frac{I+A}{2} \quad (6)$$

$$\omega = \frac{\chi^2}{2\eta} \quad (7)$$

S/No. Name of compound	Optimized structure	Homo orbital	Lumo orbital	f+	f-
Abemaciclib	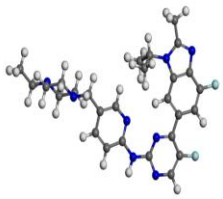	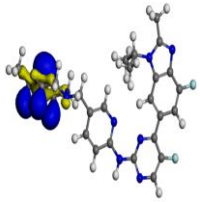	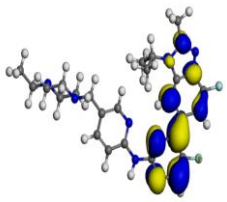	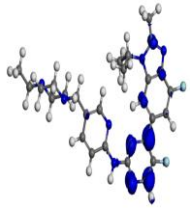	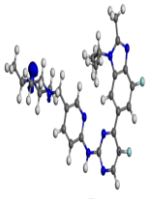
Cyclohexadecane, 1,2-diethyl-	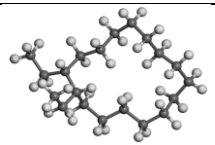	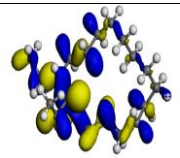	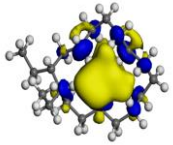	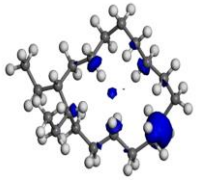	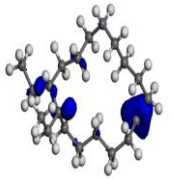
1H-Indole-2-carboxylic acid, 6-(4-ethoxyphenyl) -3-methyl-4-oxo-4,5,6 ,7-tetrahydro-, isopropyl ester	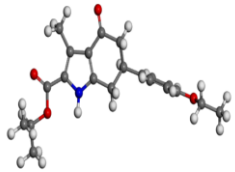	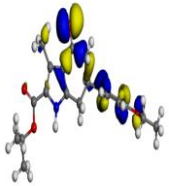	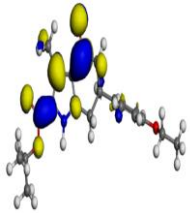	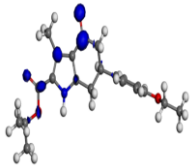	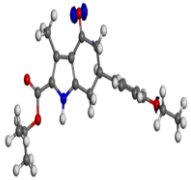
Catechin	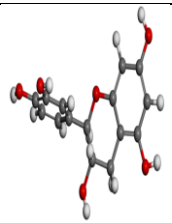	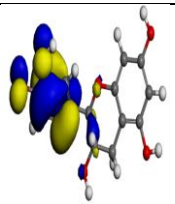	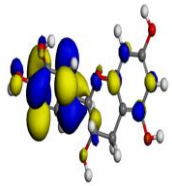	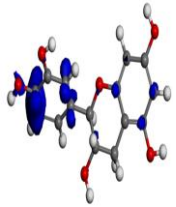	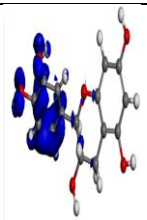

Cyclopenteno[4.3-b]tetrahydrofuran, 3-[(4-methyl-5-oxo-3-phenylthio) tetrahydrofuran-2-yloxymethylene]-	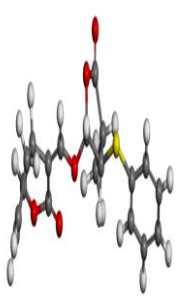	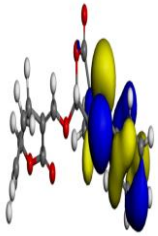	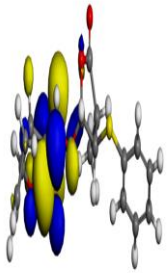	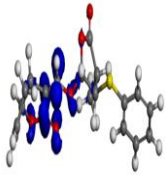	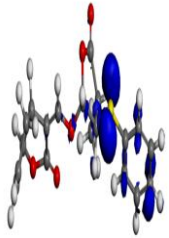
Lunamarin	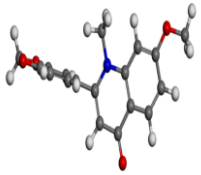	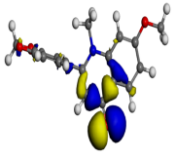	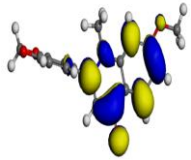	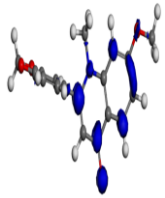	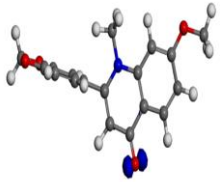

Fig. 5. optimized structures, HOMO and LUMO orbitals, funki functions of the selected compounds

Table 6. Quantum chemical descriptors of the selected compounds

Name of compound	HOMO energy (Ev)	LUMO energy (Ev)	ΔE (Ev)	I (Ev)	A (Ev)	η (Ev)	$\delta\ (Ev)^{-1}$	χ (Ev)	ω (Ev)
Abemaciclib	-5.051	-2.486	2.565	5.051	2.486	1.2825	0.7797	3.7885	5.5956
Cyclohexad ecane, 1,2-diethyl-	-6.642	-0.854	5.788	6.642	0.854	2.8940	0.3455	3.7480	2.4270
1H-Indole-2-carboxylic acid, 6-(4-ethoxyphenyl) -3-methyl-4-oxo-4,5,6 ,7-tetrahydro-, isopropyl ester	-5.116	-1.902	3.214	5.116	1.902	1.6070	0.6223	3.5090	3.8311
Catechin	-4.832	-0.707	4.125	4.832	0.707	2.0625	0.4848	2.7695	1.8594
Cyclopenteno[4.3-b]tetrahydrofuran, 3-[(4-methyl-5-oxo-3-phenylthio) tetrahydrofuran-2-yloxymethylene]-	-5.447	-2.423	3.024	5.447	2.423	1.5120	0.6614	3.9350	5.1204
Lunamarin	-4.740	-1.860	2.880	4.740	1.860	1.4400	0.6944	3.3000	3.7813

4. CONCLUSION

The compounds contained in *Curcuma longa* were extracted using ethanol and chloroform separately, the phytochemical contents were estimated by GC-MS method. Molecular docking procedure was used to investigate the compounds for their cancer inhibition properties, the result revealed that Cyclohexadecane, 1,2-diethyl-, lunamarin and Cyclopenteno[4.3-b]tetrahydrofuran, 3-[(4-methyl-5-oxo-3-phenylthio) tetrahydrofuran-2-yloxymethylene]-showed the best inhibiting properties towards 4oar cancer protein whereas, lunamarin showed the best binding power towards the 4zau cancer protein and Benzo[h]quinoline, 2,4-dimethyl-showed the best inhibiting potential towards 2dsd cancer protein. The drug likeness study using swissADME software showed that the compounds exhibited drug friendly properties none showed more than one violation of Lipinski's rule of five, the density functional theory calculations indicated that all the compounds had comparable energy gaps which is a good indication of their reactivity towards the drug targets, the results of the findings showed that *Curcuma longa* could be a good inhibitor of cancer growth and therefore isolation and critical study of its constituents are encouraged.

DISCLAIMER (ARTIFICIAL INTELLIGENCE)

Authors hereby declare that NO generative AI technologies such as Large Language Models (ChatGPT, COPILOT, etc.) and text-to-image generators have been used during the writing or editing of this manuscript.

FUNDING

This project was spnosored by The Tertary Education Trust Fund (TETFund) under the TETFund reference number TETF/DR&D/CE/UNI/IMO/IBR/2020/VOL.1

COMPETING INTERESTS

Authors have declared that no competing interests exist.

REFERENCES

1. Piña-Sanchez P, Chavez-Gonz A, Ruiz-Tachiqu´ın M, Vadillo E, Monroy-Garc´ıa A, Montesinos J J, Grajales R, Barrera MG, Mayani H. Cancer biology, epidemiology, and treatment in the 21st century: Current status and future challenges from a biomedical perspective. Cancer Control. 2021;28:1–21.
DOI: 10.1177/10732748211038735.
2. Hickey R, Vouche M, Sze D Y et al. Cancer concepts and principles: Primer for the interventional oncologist-Part II. J Vasc Intervent Radiol. 2013;24(8):1167-1188.
3. Hanahan D, Weinberg R A, Hallmarks of cancer: The next generation. Cell. Pubmed. 2011;144(5):646-674.
4. Novikov NM, Zolotaryova SY, Gautreau AM, et al., Mutational drivers of cancer cell migration and invasion. Br J Cancer. 2021;124:102–114.
Available:https://doi.org/10.1038/s41416-020-01149-0
5. Sekhoacha M, Riet K, Motloung P, Gumenku L, Adegoke A, Mashele S. Prostate cancer review: Genetics, diagnosis, treatment options, and alternative approaches. Molecules. 2022; 5(27)17:5730.
DOI: 10.3390/molecules27175730.
PMID: 36080493;
PMCID: PMC9457814.
6. Sultana R, Islam M, Haque A, Evamoni F, Imran Z M, Khanom J, Munim M A. Molecular docking based virtual screening of the breast cancer target NUDT5. Biomedical Informatics. 2019;15(11):784-789.
7. Bray F, et al. Global cancer statistics 2018: GLOBOCAN estimates of incidence and mortality worldwide for 36 cancers in 185 countries CA Cancer. J Clin. 2018;68: 394.
[PMID: 30207593]
8. Agu PC, Afukwa CA, Orji OU, Ezeh EM, Ofoke IH, Ogbu CO, Ugwuja EI, Aja PM. Molecular docking as a tool for the discovery of molecular targets of nutraceuticals in diseases management. Scientific Reports. 2023;13:13398.
Available:https://doi.org/10.1038/s41598-023-40160-2.
9. Bairagi GR, Patel VP. Nutraceutical a review on basic need, classifcation, recent trends in industry and delivery systems. J. Emerg. Technol. Innov. Res. (JETIR). 2021;8(5):c183–c199.
10. Mardirossian N, Head-Gordon M, Thirty years of density functional theory in computational chemistry: An overview and extensive assessment of 200 density functionals. Molecular
Physics. 2017;115(19):2315–2372.

Available:https://doi.org/10.1080/00268976.2017.1333644

11. Bocci G, Carosati E, Vayer P, Arrault A, Lozano S, Cruciani G. ADME-space: A new tool for medicinal chemists to explore ADME properties. Sci. Rep. 2017;7:6359. [CrossRef] [PubMed]
12. Pantaleão SQ, Fernandes PO, Gonçalves JE, Maltarollo VG, Honorio KM. Recent advances in the prediction of pharmacokinetics prope properties in drug design studies: A review. Chem Med Chem. 2022;5(17)1. 202100542.
13. Dulsat J, López-Nieto B, Estrada-Tejedor R, Borrell J I. Evaluation of free online ADMET tools for academic or small biotech environments. Molecules. 2023;28:776.
Available:https://doi.org/10.3390/molecules28020776.
14. Issa NT, Wathieu H, Ojo A, Byers SW, Dakshanamurthy S. Drug metabolism in preclinical drug development: A survey of the discovery process, toxicology, and computational tools. Curr. Drug Metab. 2017;18:556–565.
[CrossRef] [PubMed] Sciences: Bethesda, MD, USA, 2004.
15. Adindu CB, Kalu GI. Elucidation of potential inhibitor compounds from zingiber officinale against migraine headache. WNOFNS. 2024;55:184-205.
16. Adindu CB, Kalu GI, Ikezu UJM, Ikpa CBC, Okeke PI. Molecular docking, ADMET & DFT predictions of cinnamomum zylanicum for prostate cancer inhibition. Journal of Materials Science Research and Reviews. 2024;7(3):392-426.
17. Adindu CB. In-silico screening of lung cancer inhibiting potential of the chemical constituents of N-Hexane Extract of Elaisi guineenses. Journal of Materials Science Research and Reviews. 2023;6(3):572-582.
18. Duru CE, Duru AI, Adegboyega AE. In silico identification of compounds from Nigella sativa seed oil as potential inhibitors of SARS-CoV-2 targets. Bulletin National Research Centre. 2021;45: 57.
Available:https://doi.org/10.1186/s42269-021-00517-x.
19. Petit-Topin I, Fay M, Resche-Rigon M, Ulmann A, Gainer E, Rafestin-Oblin M E, Fagart J. Molecular determinants of the recognition of ulipristal acetate by oxo-steroid receptors. The Journal of Steroid Biochemistry and Molecular Biology. 2014;144:427–435.
DOI:10.1016/j.jsbmb.2014.08.008 .
20. Yosaatmadja Y, Silva S, Dickson JM, Patterson A V, Smaill JB, Flanagan JU, Squire CJ. Binding mode of the breakthrough inhibitor AZD9291 to epidermal growth factor receptor revealed. Journal of Structural Biology. 2015;192(3):539–544.
DOI: 10.1016/j.jsb.2015.10.018
21. Zha M, Zhong C, Peng Y, Hu H, Ding J, Crystal structures of human NUDT5 reveal insights into the structural basis of the substrate specificity. Journal of Molecular Biology. 2006;364(5):1021–1033.
DOI:10.1016/j.jmb.2006.09.078.
22. Johnson RD, et al. Abemaciclib plus endocrine therapy for hormone receptor-positive, HER2-negative, node-positive, high-risk early breast cancer (monarchE): Results from a preplanned interim analysis of a randomised, open-label, phase 3 trial. The Lancet Oncology. 2023;24(1):77-90.
23. SC, DK S, Ragunathan V, Tiwari P, AS, P BD. Molecular docking, validation, dynamics simulations, and pharmacokinetic prediction of natural compounds against the SARS-CoV-2 main-protease. J Biomol Struct Dyn. 2022 Feb;40(2):585-611.
DOI: 10.1080/07391102.2020.1815584.
Epub 2020 Sep 8.
PMID: 32897178;
PMCID: PMC7573242.
24. Diana A, Michielin O, Zoete VA, SwissADME: A free web tool to evaluate pharmacokinetics, drug likeness and medicinal chemistry friendliness of small molecules. Scientific Reports. 2017;7:42717.
DOI: 10.1038/srep42717,
25. Potts RO, Guy RH. Predicting skin permeability. Pharm. Res. 1992;9:663–669.
26. Ritchie TJ, Macdonald JFS. Peace S, Pickett SD, Luscombe CN. Increasing small molecule drug developability in suboptimal chemical space. Royal Society of Chemistry. 2013;4:1-8.
27. Daina A, Zoete VA. BOILED-Egg to predict gastrointestinal absorption and brain penetration of small molecules. Chem Med Chem. 2016;11:1117–1121.
28. Oguzie EE, Ogukwe CE, Ogbulie JN, Nwanebu FC, Adindu CB, Udeze IO, Oguzie KL, Eze FC. Broad spectrum

corrosion inhibition: Corrosion and microbial (SRB) growth inhibiting effects of Piper guineense extract. Journal of Material Science. 2012;47:3592–360.

29. Hussein RK, Elkhair HM, Elzupir AO, Ibnaouf KH. Spectral, structural, stability characteristics and frontier molecular orbitals of tri-n-butyl phosphate (tbp) and its Degradation Products: DFT calculations. J. Ovonic Res. 2021;17:23–30.
30. Deghady AM, Hussein RK, Alhamzani AG, Mera A. Density functional theory and molecular docking investigations of the chemical and antibacterial activities for 1-(4-Hydroxyphenyl)-3- phenylprop-2-en-1-one. Molecules. 2021; 26:3631. Available:https://doi.org/10.3390/molecules26123631.
31. Nesereen TM, Ahmed MA, Rageh KH, Moez AI, Abdulrahman GA, Mortage MA, DFT, ADMET and Molecular Docking Investigations for the Antimicrobial Activity of 6,6′-Diamino-1,1′,3,3′-tetramethyl-5,5′-(4-chlorobenzylidene)bis[pyrimidine-2,4(1H,3H)-dione], Molecules. 2022; 27(3): 620. Available:https://doi.org/10.3390/molecules27030620

Peer-review history:
The peer review history for this paper can be accessed here:
https://www.sdiarticle5.com/review-history/125919